CONTROLLING TURBULENCE IN REACTION DIFFUSION SYSTEMS

Shawn D. Pethel, and Ned J. Corron
U. S. Army Research, Development and Engineering Command
Aviation and Missile Research, Development and Engineering Center
Redstone Arsenal, Alabama 35898

ABSTRACT

We propose local symbolic models as a practical tool for understanding high-dimensional spatiotemporal chaos in reaction-diffusion systems modeled by coupled map lattices (CMLs). A local symbolic model is a truncation of the full symbolic dynamics to one that considers only a single element and a few neighbors. Local symbolic models can be applied element by element to a large lattice to build up an approximate picture of the global dynamics. Whereas the difficulty of finding the exact global symbolic dynamics increases exponentially with lattice size, the difficulty of the approximation presented here increases linearly at worst. The many uses of symbolic dynamics for one-dimensional maps, including control and targeting, are thus made practical for lattices. We explore the efficacy of the concatenated local model approach and give an example of controlling an arbitrary pattern in a CML using only small perturbations.

1. INTRODUCTION

In this Letter, we approximate the global symbolic dynamics of a coupled map lattice (CML) with a set of local models each using only a small number of symbols. Coupled map lattices [Kaneko, 1990] are popular models of spatiotemporal chaos in reaction diffusion systems and their description via symbolic dynamics may provide an efficient and rigorous basis for understanding them. Indeed, the topology of unimodal maps has been completely elucidated in terms of 2-symbol alphabets [Kitchens, 1998], and recently it has been conjectured that these results extend simply to the CML case [Pethel, 2006]. Nevertheless, one still has to contend with the issue of dimensionality in lattices. While a single logistic map is fully described by 2 symbols, an N-element lattice of them requires an alphabet of 2^N symbols. Manipulation of the global symbolic dynamics of a large lattice would therefore appear impractical. In the case of nearest neighbor coupling, however, we show that the dynamics at any particular site is well-approximated by a much smaller local symbolic model that is independent of lattice size. This property leads us to propose representing the global symbolic dynamics as a collection of local models, one per site. The appeal of this approach is that is it computationally tractable: because the local models are fixed in size, storage for the whole collection scales linearly with N. Furthermore, CMLs of identical maps with periodic boundaries require only one local model. Here we report on the efficacy of local symbolic models compiled from data and apply them to the problem of controlling spatiotemporal chaos in a CML.

2. SYMBOLIC DYNAMICS OF CMLS

We consider a map lattice with N sites labeled $i = 1 \ldots N$. Each site is described by a state x_t^i in the interval I^i and a unimodal local dynamic $f_i : I^i \to I^i$. Denote by F the product function of f_i onto each site, and by A an $N \times N$ coupling matrix, then the map lattice can be written as $\vec{x}_{t+1} = H(\vec{x}_t)$, where $H = A \circ F$. Models of this type have been extensively studied with regard to turbulence and pattern formation [Kaneko, 1985]. Here we wish to introduce an alternate formulation in terms of local symbolic dynamics.

As reported previously [Pethel, 2006], it is conjectured that for A nonsingular a homeomorphism exists between the spatiotemporal sequence $\{x_t^i : i = 1 \ldots N, t \geq 0\}$ and the equivalently sized set of binary symbols s_t^i defined by

$$s_t^i = \begin{cases} 0 & if \quad x_t^i \in I_0^i \\ 1 & if \quad x_t^i \in I_1^i \end{cases} \tag{1}$$

where I_0^i and I_1^i are the two sub-intervals over which the unimodal map f_i is monotonic. Figure 1a,b illustrates this mapping for a CML of logistic maps. The particular state x_t^i is homeomorphic to s_t^i plus the set $\{s_l^j : j = 1 \ldots N, l > t\}$. This relationship can be understood in the following way. Consider that the symbol vector $\vec{s}_{t+n}$ indicates which sub-interval the components of $\vec{x}_{t+n}$ lie in. Provided one knows which preimage to use, an estimate for $\vec{x}_{t+n-1}$ can obtained by applying H^{-1} onto this vector of sub-intervals. The symbol vector $\vec{s}_{t+n-1}$ identifies the correct preimage because the two preimages of f_i lie on different monotonic segments. We repeat this process until an estimate of $\vec{x}_t$ is reached. At the last step only the symbol s_t^i is required to estimate x_t^i. Because

Report Documentation Page

Form Approved
OMB No. 0704-0188

1. REPORT DATE	2. REPORT TYPE	3. DATES COVERED
01 NOV 2006	**N/A**	**-**

4. TITLE AND SUBTITLE	5a. CONTRACT NUMBER
Controlling Turbulence In Reaction Diffusion Systems	5b. GRANT NUMBER
	5c. PROGRAM ELEMENT NUMBER
6. AUTHOR(S)	5d. PROJECT NUMBER
	5e. TASK NUMBER
	5f. WORK UNIT NUMBER
7. PERFORMING ORGANIZATION NAME(S) AND ADDRESS(ES) **U. S. Army Research, Development and Engineering Command Aviation and Missile Research, Development and Engineering Center Redstone Arsenal, Alabama 35898**	8. PERFORMING ORGANIZATION REPORT NUMBER
9. SPONSORING/MONITORING AGENCY NAME(S) AND ADDRESS(ES)	10. SPONSOR/MONITOR'S ACRONYM(S)
	11. SPONSOR/MONITOR'S REPORT NUMBER(S)

12. DISTRIBUTION/AVAILABILITY STATEMENT
Approved for public release, distribution unlimited

13. SUPPLEMENTARY NOTES
See also ADM002075., The original document contains color images.

14. ABSTRACT

15. SUBJECT TERMS

16. SECURITY CLASSIFICATION OF:			17. LIMITATION OF ABSTRACT	18. NUMBER OF PAGES	19a. NAME OF RESPONSIBLE PERSON
a. REPORT **unclassified**	b. ABSTRACT **unclassified**	c. THIS PAGE **unclassified**	**UU**	**5**	

the inverse of a chaotic map is, on average, contracting, the estimate converges to x_t^i as $n \to \infty$.

In practice one uses a finite n and deals with a space of truncated symbol sequences. This truncation is analogous to using a fixed number of bits to represent the real line in a digital computer. Symbols that occur further in the future are exponentially less significant than symbols that occur earlier in the temporal sequence. The total number of symbols representing x_t^i is, then, $Nn+1$. Thus to construct an explicit mapping between the CML site value and the symbolic states one has to account for as many as 2^{Nn+1} possibilities, which is impractical for large lattices.

3. THE LOCAL SYMBOLIC MODEL

The theme of this Letter is that the symbolic model can be truncated spatially as well as temporally. If the coupling matrix A is tridiagonal or cyclic tridiagonal with a dominant diagonal---i.e. the CML employs diffusive nearest neighbor coupling---then symbols that appear at sites further away from the point of interest have exponentially less influence than those that occur nearby. As described above, the symbols are related to the CML state via repeated applications of the inverse mapping $H^{-1} = F^{-1} \circ A^{-1}$. In the case that A is tridiagonal the elements of A^{-1} can be found analytically [Yamani, 1997] and shown to fall off exponentially in magnitude with increasing offset from the diagonal. The exponential decline in significance of the off-diagonal terms is our basis for truncating the symbols spatially as well as temporally. In the rest of this Letter we will concern ourselves with a minimal local symbolic model of the dynamics at site i that only considers symbols at that site plus its two neighbors (Fig. 1c). Importantly, the local model restricted in this way requires only $3n+1$ symbols and is therefore independent of the lattice size N.

We define a local symbolic model as the set S^i of at most 2^{3n+1} elements representing all truncated symbol patterns that are allowed by the dynamics at site i. By ``pattern" we mean a particular arrangement of symbols within the $3n+1$ paddle-shaped window (Fig. 1c). A *global* symbolic state $\Sigma_{k_1 \cdots k_N} = S_{k_1}^1 S_{k_2}^2 \ldots S_{k_N}^N$ is an overlapping concatenation of local symbolic states. An overlapping concatenation is possible between two local symbolic states only if overlapping symbols match. The approximated global symbolic dynamic can now be defined as the set $\{\Sigma_{k_1 \cdots k_N}\}$ of all overlapping concatenations of local symbolic states. Obviously, any incompatibilities that occur outside the spatial and temporal boundaries of the local model are not accounted for in this approximation. The set $\{\Sigma_{k_1 \cdots k_N}\}$ as defined above is therefore a superset of the actual global symbolic model.

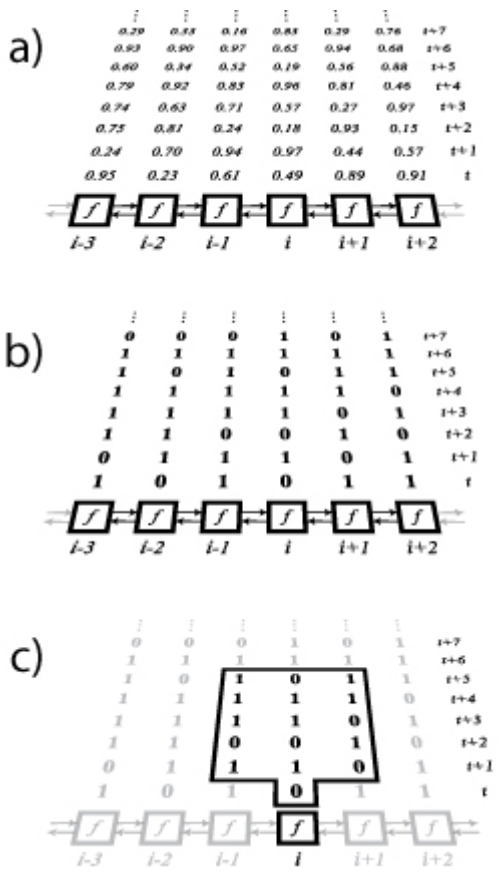

Fig. 1 A time-space segment of a 1-d CML of logistic maps. A) Real valued CML states shown with 2 digits of precision, b) the equivalent symbolic representation, c) the local symbolic model using $n=5$.

The local models give us a tractable means of describing the global symbolic dynamics of the CML. If we define the complexity of a set to be its cardinality, then the maximum complexity of the entire collection of local models is $N \cdot 2^{3n+1}$. This extreme assumes no symmetry is present in the CML and a different local model must be used at each site. The difficulty, then, of approximating the global symbolic dynamics using truncated local models scales at worst linearly with N, whereas the exact symbolic description scales exponentially.

4. EXAMPLE CASE

Having defined our local model approach, we wish to investigate its efficacy in terms of the commonly studied CML written as

$$x_{t+1}^{i} = (1-\varepsilon) f(x_t^i) + \frac{\varepsilon}{2}\left[f(x_t^{i-1}) + f(x_t^{i+1}) \right] \qquad (2)$$

along with rules for the boundary sites [Kaneko, 1990]. The coupling parameter $\varepsilon \in [0,0.5]$ sets the diffusion rate. For large N the off-diagonal terms of A^{-1} decay in magnitude as $(\varepsilon/(2-2\varepsilon)^{|\delta|}$, where δ is the offset from the diagonal [Yamani, 1997]. For our example case we choose the moderate coupling strength $\varepsilon = 0.1$ and $N = 1000$ elements. The restriction of the local model to nearest neighbor symbols is tantamount to neglecting the $\delta \geq 2$ elements of A^{-1}, which are less than 1% of the diagonal terms.

Staying with convention we use the logistic map $f(x) = 4x(1-x)$ as the local dynamic; therefore, the symbol "0" corresponds to a state value in the interval $I_0 = [0,0.5)$ and the symbol "1" to the interval $I_1 = [0.5,1]$. Here the local dynamic is the same everywhere and, when periodic boundaries are used, the coupling topology is uniform across the array. This arrangement is optimal in the sense that one need only store a single local model and re-use it at each site in the array. In this case, the difficulty of applying our method does not increase with the size of the CML.

Our strategy for obtaining the local model is to compile it from time series data and to rely on the ergodic properties of chaos to survey the local topology. In principle, an exact topology is computable using a pruning front method [Pethel, 2006, Cvitanovic, 1988], but the details have yet to be developed for this case. We find the time series approach to be a practical alternative albeit less rigorous. A drawback is that transients and rare orbits will not be fully represented in a finite time observation. The global symbolic model $\{\Sigma_{k_1 \cdots k_N}\}$ assembled this way is an approximation of the actual dynamics, not a true superset.

Our local symbolic model is generated in three steps. First, the CML is iterated 10^5 times starting from a random initial condition. Second, the 10^8 $(N \times 10^5)$ CML site values are mapped to symbols using (1). Finally, at each spatiotemporal index (i,t) two items are recorded: the paddle-shaped window of symbols who's "handle" is located at (i,t), and the CML site value x_t^i . All unique symbol patterns are recorded in the set S and the corresponding site values in the set T (Fig. 2). When multiple site values are found for the same symbol pattern, the mean is taken. The pair (S,T) serves as a look-up table (LUT) relating the symbol pattern to the CML state that produces it; this is the practical record of the commuting function that carries symbolic states to spatial states.

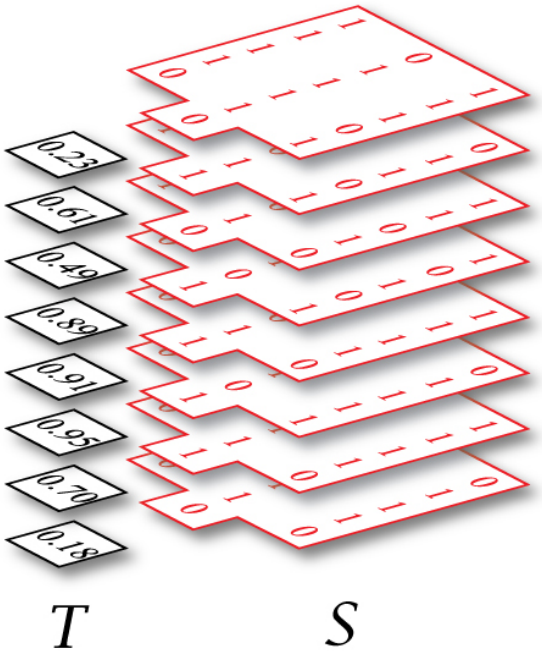

Fig.2 An illustration of the sets S and T for $n = 5$.

5. RESULTS

We gauge the fidelity of the local symbolic model by comparing it against a new data set of 10^5 iterations. The test data is symbolized and the LUT used to produce an expected state value for each site at each time step. The absolute error between the expected value and the known value is computed for each data point. In Table 1 we report the mean and the maximum absolute error over the entire data set for $n = 1$ to 7 along with the number of patterns in the local model. These errors should be compared to the $[0,1]$ range of the dynamics at each site. For each case different data sets were used for the creation and testing of the model.

n	Patterns	Mean abs error	Max abs error
1	16	0.0682	0.2146
2	119	0.0384	0.1511
3	620	0.0246	0.1427
4	3,265	0.0152	0.0926
5	16,036	0.0101	0.0895
6	74,405	0.0067	0.0736
7	331,368	0.0048	0.0689

Table 1 Model size and absolute error versus n

As expected, the fidelity of the local model improves with increasing temporal cutoff n. The behavior of the mean absolute error is well tracked by the function $E(n) = \alpha e^{-\lambda n} + \beta$, with parameter values $\alpha = 0.1145$, $\lambda = 0.5712$, and $\beta = 0.0032$ (determined by least squares fitting). The improvement in mean error must be weighed against an exponential growth in the number of patterns stored by the model as well as the existence of a non-zero error floor. We attribute the error floor ($\beta = 0.0032$) to the error inherent in truncating the local symbolic model to include only nearest neighbors. Using the same methodology the floor for the maximum absolute error extrapolates to 0.051.

In the above analysis, missing symbol patterns in the LUT were ignored. This situation occurs when the test data contains a rare symbol pattern that was not in the data used to assemble the LUT. In all cases missing patterns represented far less than 1 percent of the test data. Rare patterns were numerous in variety: Fully half of the $n = 7$ LUT is comprised of patterns that, in total, account for less than 3% of the dynamics, and almost 8% of the LUT content appeared only once in the training data.

Aside from fluctuations in rare content, the bulk of the symbol patterns were found to be remarkably consistent across lattices of different sizes. In fact, the LUT compiled for the case N=1000 *performs equally well for any* N>2. This robustness is no doubt due to the topological nature of the symbolic description and to the nearest neighbor truncation. The global behavior for different initial conditions and different N is always restricted to what is allowed by the local topology. Unlike the global CML attractor, the smaller state space of the local dynamics can be adequately covered in a short time observation.

6. CONTROLLING TURBULENCE

If we are satisfied with the fidelity of the local model, then the full power of a symbolic dynamical description of the CML is available to us. This includes construction of global trajectories (not just states) via temporal concatenation of the local models. The number of possible combinations is vast, but it is straightforward to target orbits with particular properties, such as periodicity [Pethel, 2006]. A taxonomy of behaviors seen in large CMLs [Willeboordse, 2002] could be built on this basis. Here we do not address this important topic, but turn to a related issue---that of controlling spatiotemporal chaos.

Within the framework of symbolic dynamics, targeting and control of chaos is straightforward [Hayes, 1993, Corron, 2003]. Using local symbolic models equivalent methods can be employed to target and control high dimensional chaos in CMLs. Once a symbolic trajectory is formulated, the real valued CML states can

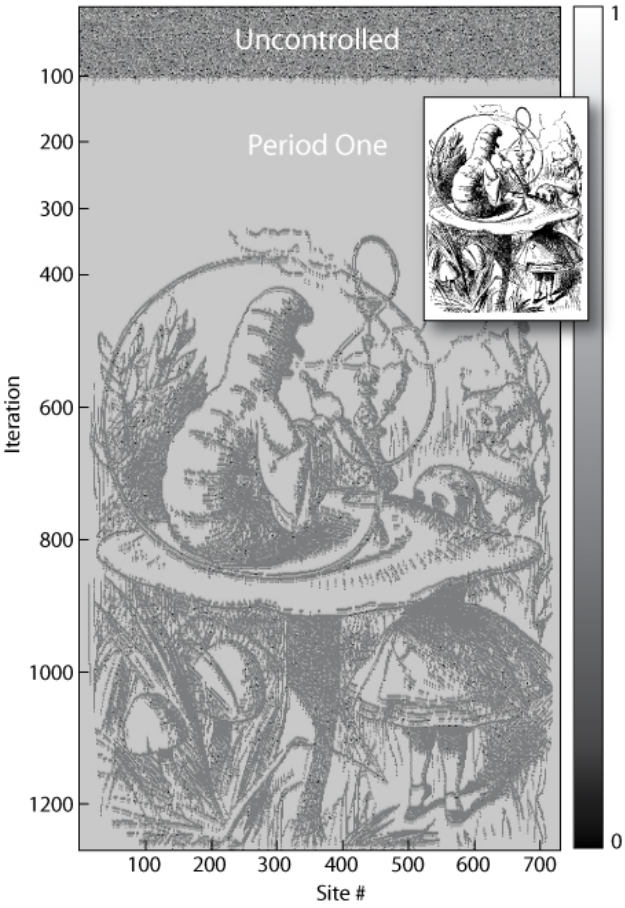

Fig.3 A time-space plot of a 1-d CML of 726 logistic maps. CML site values are shown on a compressed grayscale. Prior to iteration 100 the CML is uncontrolled. At iteration 100 control is initiated. By iteration 112 the CML has reached the uniform period one state. At iteration 300 a complex orbit is targeted that approximated the image shown in the overlay.

be read from the LUT as described previously and fed into a controller. An example is illustrated in Fig.3 of targeting the uniform period one state starting from an uncontrolled CML of N=726 logistic maps ($\varepsilon = 0.1$). At iteration 100 a new symbolic state is formed by creating an $N \times 8$ symbolic representation of the uncontrolled CML state and overwriting the least significant row with all “1”s. The CML site values corresponding to this new symbolic state are read from the $n = 7$ LUT (taken from the N=1000 case) and differenced with the current CML state. This difference vector is the control signal used to force the CML onto the new state. Because only least significant symbols are altered these perturbations are small. At each subsequent time step the process is repeated and the CML rapidly approaches the uniform period one orbit represented symbolically by “1”s at every site. During targeting the average control perturbation is found to be 0.0031, which is consistent with the expected

fidelity of the $n = 7$ local symbolic model. At some sites a symbolic transition was encountered that was not allowed by the dynamics or was simply missing from the LUT. In these cases the rogue element was allowed to roam uncontrolled until it came within a distance of 0.025 of the target trajectory. At that point it was forced onto the desired state. More sophisticated targeting algorithms can also be applied here [Bollt, 1998].

The primitive targeting method applied above is serviceable for more complex trajectories as well. Inspired by the notion that the local symbol patterns could be assembled into a recognizable image, we chose a line drawing as a target trajectory. The drawing, shown as an inset in Fig. 3, is a 480 x 363 black and white image from the book "Alice's Adventures in Wonderland" [Carrol, 1865]. The black and white pixels are interpreted as "0" and "1" symbols, respectively. A preliminary analysis shows that this image is largely incompatible with the $n = 7$ LUT, primarily because the CML dynamics do not allow long blocks of "0"s (dark areas). This problem was overcome by doubling the dimensions of the image to 960 x 726 and replacing every black pixel with a 2x2 checkerboard of white and black pixels, thereby eliminating any block of consecutive "0"s. The larger image was found to be 97% consistent with the LUT. As shown in Fig. 3, this complex orbit was targeted from the previously controlled uniform period one state. Again, the mean control signal was small (0.0027) with a maximum of 0.025 due to the 3% of the image that is incompatible with the CML dynamics.

7. CONCLUSION

These examples indicate that modeling and controlling global motion in coupled map lattices is computationally feasible when using local symbolic models. The primary trade off is between the fidelity of the local model and the number of symbol patterns that must be stored, which grows exponentially with the size of the local neighborhood. For clarity of presentation no optimizations were employed to further reduce the size of the local model, although some are evident \cite{optimization}. The CML architecture used here is of the simplest form, but the authors believe the local model approach can be generalized with similar effectiveness to other configurations. Given the relevance of CMLs to a wide variety of spatiotemporal chaotic phenomena, it is plausible that the method presented here can be adapted to understand and control turbulence in a reaction diffusion system.

REFERENCES

Bollt, E. and E. Kostelich, 1998: Optimal targeting of chaos, *Phys. Lett. A. 245*, 399-406.

Carrol, L., 1865: Alice's Adventures in Wonderland. Project Gutenberg, www.gutenberg.org

Corron, N. J.and S. D. Pethel, 2003: Experimental targeting of chaos via controlled symbolic dynamics, *Phys. Lett. A. 313*, 192-197.

Cvitanovic, P., G. H. Gunaratne, and I. Procaccia, 1988: Topological and metric properties of Henon-type strange attractors, *Phys. Rev. A* 38, 1503-1520.

Hayes, S., C. Grebogi, and E. Ott, 1993: Communicating with chaos, *Phys. Rev. Lett.* 70, 3031-3034.

Kaneko, K., 1985: Spatiotemporal Intermittency in Coupled Map Lattices, *Prog. Theo. Phys*. 74, 1033-1044.

Kaneko, K., 1990: *Formation, Dynamics, and Statistics of Patterns*. World Scientific.

Kitchens, B. P., 1998: *Symbolic Dynamics*. Springer.

Pethel, S. D., N. J. Corron, and E. Bollt, 2006: Symbolic Dynamics of Coupled Map Lattices, *Phys. Rev. Lett.* 96, 034105.

Willeboordse, F. H., 2002: Hints for universality in coupled map lattices, Phys. Rev. E 65, 026202.

Yamani, H. A. and M. S. Abdelmonem, 1997: The analytic inversion of any finite symmetric tridiagonal matrix, *J. Phys. A: Math. Gen*. 30, 2889-2893.